ANALYSIS OF ATMOSPHERIC EFFECTS ON X-BAND SYNTHETIC APERTURE RADAR OBSERVATIONS AND PRECIPITATIONS ESTIMATION

S. Mori [(1)], L. Pulvirenti [(1)], F.S. Marzano [(1,2)], and N. Pierdicca [(1)]

[(1)] Dept. Information Eng., Electronics and Telecommunications, Sapienza University of Rome, via Eudossiana 18, 00184 Rome (Italy), mori@diet.uniroma1.it
[(2)] CETEMPS, University of L'Aquila, L'Aquila, Italy

ABSTRACT

This paper proposes a new methodology for the detection and quantitative estimation of intense atmospheric precipitations on images acquired by Synthetic Aperture Radars (SARs) operating at X-Band wavelengths. The proposed methodology consists of two successive steps. The first one allows detecting and distinguishing areas subjected to intense precipitation events, permanent water surfaces, flood areas and snow coverage. The second step derives an estimation of the precipitation rate using the event attenuation estimated at the previous step. This methodology is applied on two COSMO-SkyMed (CSK) satellite case studies. The first one is relative to a severe precipitation weather event, occurred in northwestern Italy (close to Liguria region) on November 3-8, 2011. The second one is relative to Hurricane "Irene" event, occurred in Eastern United States (close to Delaware) on late August 2011. In both cases X-SAR echoes and estimated rain rate is compared with corresponding products derived by available ground Weather Radars (WRs). The correlation of the precipitating cloud fields between CSK X-SAR and WR images is significant in all case studies.

1. INTRODUCTION

Global climate change is of increasing interest both for public opinion and scientific community, due to its implications on global economy and human communities, as proved by numerous disasters occurred worldwide in recent years caused by severe weather events. In this perspective models for analysis and weather forecasting acquire importance; unfortunately the same require high spatial resolution data to be assimilated. A recent possibility is represented by Spaceborne Synthetic Aperture Radars (SARs) operating at X-Band, that allow high resolution also in remote or orographic areas where other measurements are not available. Several authors have reported the sensitivity of X-SAR amplitude and phase signals to precipitation events (e.g. [1], [2], [3]). X-SAR potentialities have been attested also by a model approach [4]. Indeed, the exploitation of X-SAR observations for quantitative precipitation retrieval is still at an early stage and far from being fully assessed and demonstrated. Stimulating perspectives are offered by the recent deployment of the COSMO-SKyMed satellite constellation [5] and of and TanDEM-X/TerraSAR-X satellites [6], respectively by Italian Space Agency (ASI) and by Deutsches zentrum fur Luft und Raumfahrt (DLR); actually a similar presence of spaceborne X-SARs allows to partially overcome the reduced duty cycle of these instruments, one of their principal limitation to natural events observation. In this work two COSMO-SkyMed (CSK) case studies are analysed respect their precipitation signatures. The first case is relative to a severe precipitation weather event, occurred in north-western Italy on November 3-8, 2011. In this case CSK X-SAR data have been compared with WR reflectivity data obtained by the Italian Radar National Mosaic. The second case is relative to Hurricane "Irene" event, occurred in Eastern United States on late August 2011. CSK X-SAR images are compared with respect to concurrent ground-based S-band NEXRAD Weather Radar (WR) reflectivities.
A new methodology is applied to both case study to detect the areas affected by intense precipitation and distinguish them from flood ones; actually both areas are characterized by intense negative Normalized Radar Cross Section (NRCS) and can be confused. This methodology requires ancillary data, such as land cover maps, a digital elevation model (DEM) and spaceborne high resolution optical data (e.g. LandSAT) and as final products allows to obtain atmospheric effects free NRCSs, more precise flood maps and finally precipitations maps. In this work precipitation maps will be derived by the two study cases; the same will be compared to precipitation maps obtained by corresponding WR measurements.

2. AVAILABLE DATA

The Italian case study was foresighted as a weather hazard. CSK was programmed to continuously monitor the North-western Italy event starting from November 4, 2011 until November 8, 2011. Within the available CSK data, we have selected a Stripmap image in HH (copolar horizontal) polarization, acquired on November 5, 2011 05:15 UTC and centred at about 43.47/44.30 °N, 7.39/8.16 °E. The concurrent WR imagery has been retrieved from the Italian National Radar Mosaic data as C-Band Vertical Maximum Intensities (VMI, dBZ) [7].

Proc. 'ESA Living Planet Symposium 2013', Edinburgh, UK
9–13 September 2013 (ESA SP-722, December 2013)

Fig. 1 top panel shows the Italian Radar National Mosaic VMI at 05:15 UTC, with superimposed the MSG IR_10.8 image acquired at 05:00 UTC; the red box indicates the case study area, detailed in Fig. 1 bottom panel. Here the CSK image [dB], 10 m resolution, on the left (black colours indicate backscattering attenuation), is compared to the stretched Vertical Maximum Intensity (VMI) [10-50 dBZ], 100 m resolution, on the right, derived from the Italian Radar National Mosaic (white colours indicate higher radar reflectivity).

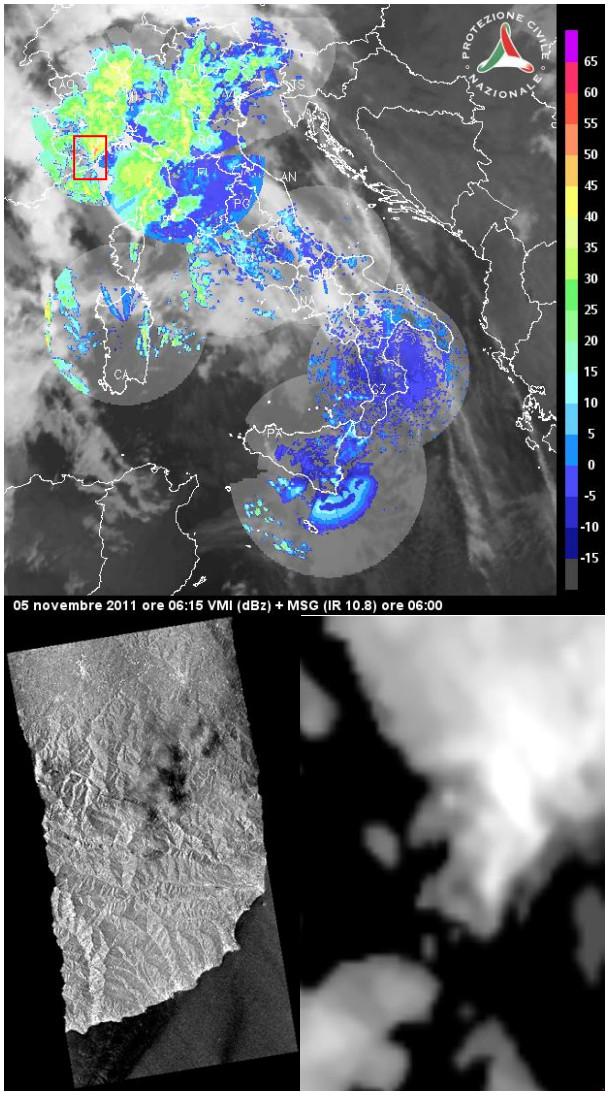

Figure 1. Liguria (IT) Event Case (November 5, 2011 – 05:15 UTC).(Top panel) Italian Radar National Mosaic Vertical Maximum Intensities (VMI) plus previous MSG IR_10.8 image; (Bottom left panel) COSMO-SkyMed (CSK) scene [dB] (corresponding to red box of top panel); (Bottom right panel) VMI detail of CSK scene.

Hurricane "Irene" was continuously monitored since its origin (i.e. [8]). Landing on U.S. east coast and approaching towards New York City was foresight and was argument of major concern. CSK X-SAR available data include a ScanSAR-Wide acquisition in HH (copolar horizontal) polarization, acquired on August 27, 2011 between 22:54:25 and 22:56:37 UTC. The acquisition covers an area along the United States northeast coast, where we have selected a portion centred at about 38.25/39.25 °N, -76.25/-74.75 °E. United States weather radar coverage is ensured by NexRad S-Band radar network [9], which includes more than 150 stations. Unfortunately for the selected event only data acquired in KDOX (38.82 °N, -75.44 °E, Dover, DE) WR site were available with an acceptable time gap (acquisition time 22:57:19 UTC). Moreover KDOX site is one of the few not upgraded to super resolution (0.5° x 250m) so its data are still at only 1° x 1000m.

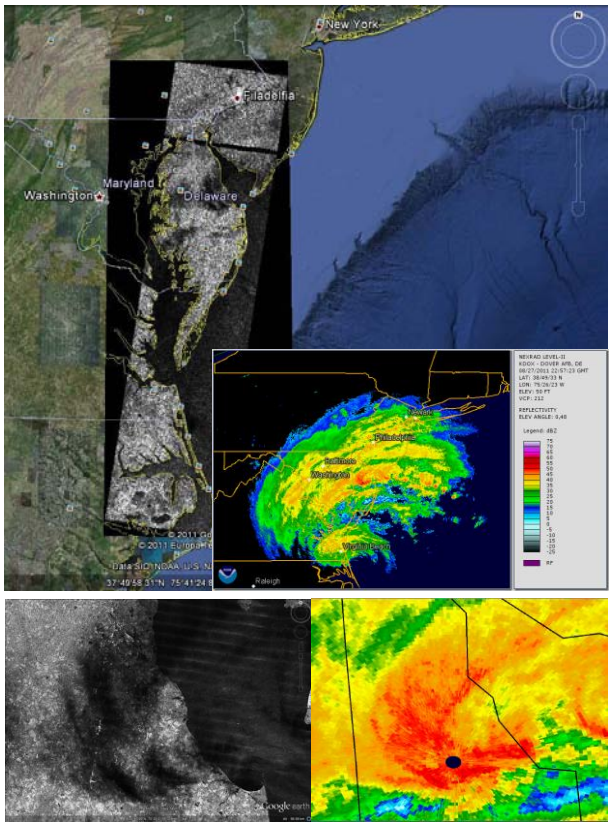

Figure 2. Hurricane "Irene" (U.S.) Event Case (August 27, 2011 - 22:55 UTC). (Top panel) CSK scene [grey levels] and corresponding Plan Position Indicator (PPI) 0.48° reflectivity [dBZ] acquired by Weather Radar (WR) KDOX site. (Bottom panel) detail of CSK (left) and WR (right) data for the reflectivity peak around the radar site (black point in figure)

Fig. 2 top panel shows the CSK scene (grey levels; black indicates backscattering attenuation) localized by mean of Google Earth® tool; the same panel show also corresponding Plan Position Indicator (PPI) 0.48° reflectivity acquired by KDOX site, processed using the NOAA WCT® tool (red colours indicate higher radar

reflectivity); bottom panel shows an enlargement of both images relative to the reflectivity peak around the radar site (black point of bottom right panel).
CSK X-SAR data have been calibrated and geocoded by means of the ENVI/SARSCAPE® software to derive the backscattering coefficient σ_{SAR}. For this purpose, we have used the Shuttle Radar Topography Mission (SRTM) DEM. Besides DEM, as ancillary data we have also used Land Cover maps derived from the European Corine Land Cover project (http://www.eea.europa.eu) and by the U.S. National Land Cover Database (http://www.mrlc.gov/index.php). In both datasets we have considered a reduced, but still significant number of macro-classes (i.e., level 2 hierarchy).

3. X-SAR RAINFALL ESTIMATION

CSK copolar horizontally-polarized backscattering coefficient σ_{SAR} [dB] and WR copolar horizontally-polarized reflectivity Z [dBZ] have been co-registered to verify the presence of atmospheric signatures within the X-SAR retrievals. As observed in previous works (e.g. [4]), the X-SAR echoes σ_{SAR} are composed by both earth surface σ^0 and volumetric atmospheric effects σ_{vol} contributions, weighted by the two-way attenuation of the precipitating cloud if present:

$$\begin{aligned} \sigma_{SAR}(x,y) &= \sigma_{srf}(x,y) + \sigma_{vol}(x,y) \\ \sigma_{srf}(x) &= \sigma^0(x) \cdot L^2\left[\Delta l(x)\right] \\ \sigma_{vol}(x) &= \sin(\theta) \cdot \int_{\Delta t(x)} \eta(t) \cdot L^2\left[\Delta l(x)\right] dt \end{aligned} \quad (1)$$

In Eq. 1, η is the radar volume reflectivity [dBZ], k the specific attenuation coefficient [dB/km], L the one-way atmospheric loss factor (dimensionless quantity between 0 and 1), θ is the off-nadir angle [deg], whereas Δl and Δt are the longitudinal (radial) and transverse path increments along l and t directions, respectively, x is the across-track direction and y is the along track one.
In this respect, X-SAR detection of rainfall is affected by the correct knowledge of the surface backscattering σ^0, especially for lighter precipitation. On the other hand, WR reflectivity is sensitive to raindrop concentrations and larger sizes, weighted by the particle size distribution and orientation. In this work we have considered WR data as ground truth for the proposed X-SAR methodology. Nevertheless differences can arise by the different wavelength and observing geometry and by phenomenon such as beam blockage and anomalous propagation affecting WR measurements. WR reflectivity Z [mm^6/m^3] can be "converted" into rain rate [mm/h] using the standard Marshall-Palmer Z-R relation $R = (Z/200)^{1/1.6}$ or the best rain-rate estimator available for the scene. More sophisticated and accurate techniques exist (e.g. [10]) but require data and instrumentations not always available. For the purposes of this work, uncertainties of Z-R methods are acceptable.
Fig. 1 and Fig. 2 show a qualitative analysis for the Italian and U.S. cases, resulting in an evident agreement for both cases between WR strong reflectivity and X-SAR backscattering attenuation. Nevertheless attenuating areas on X-SAR imagery can due to not only to precipitation but also to water surfaces, flood areas or snow coverage. The core of the proposed methodology allows discriminating precipitation signatures respect to other targets within the X-SAR image and consequently estimating the attenuation due to atmospheric effects. It consists of two distinguished steps: a first one in which areas affected by intense precipitations are detected and corresponding attenuation estimated; and a second one in which the estimated attenuation is used to derive an estimation of the precipitation rate.

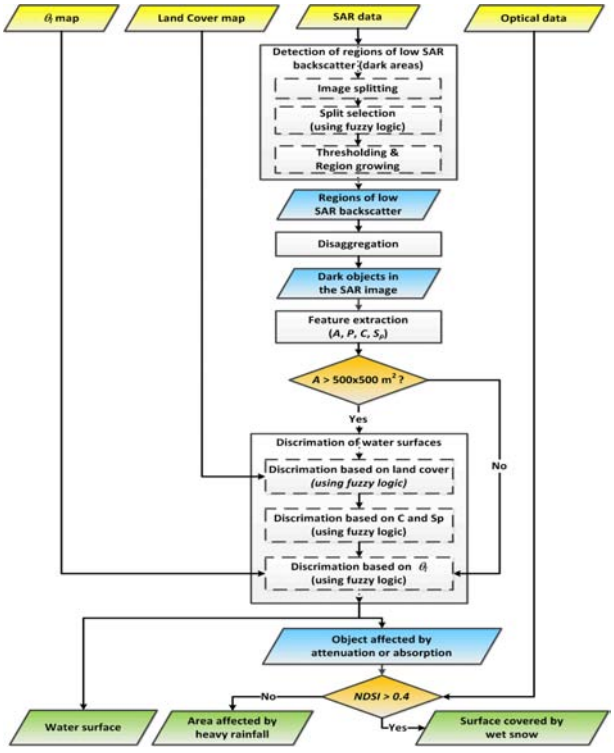

Figure 3. Block diagram of SAR Images Dark Object Classifier (SIDOC) algorithm.

The first phase of the procedure (identification on X-SAR scene of areas affected by intense precipitations) is performed by the SAR Images Dark Object Classifier (SIDOC) algorithm, shown in Fig. 3 and described in [11]. SIDOC can be considered as an automatic preprocessor to individuate on X-SAR imagery water surfaces (either permanent water bodies or flooded areas), areas subjected to heavy precipitations and snow coverage. SIDOC uses an object-based approach and applies the fuzzy logic; it consists of two main steps,

i.e., the detection of low backscatter (dark) areas and the classification of each dark object identified in the image. Ancillary data such as a digital elevation model (DEM), a land cover map, and eventually an optical image (e.g. Landsat, MODIS). Through the fuzzy logic, SIDOC integrates different rules for the detection and the classification of the dark objects in the SAR image that takes into account not only the image intensity, but also the geometrical and shape features of the objects, as well as information on land cover and topography. It is worth to notice that fuzzy rules introduce same degree of freedom that can be used to perform a more severe or a more permissive detection: in the first case areas affected by lighter rain can be unrecognized, in the second case increases the risk of false detections. In this work we have used quite restrictive parameters.

After this pre-analysis X-SAR data can be processed by applying a dedicated X-SAR rain retrieval algorithm. In this work we have used the statistical semi-empirical algorithm described in [1] and indicated as Modified Regressive Empirical Algorithm (MREA):

$$\hat{R}_{MREA}(x) = \begin{cases} \left[\frac{\Delta\sigma_{SAR}(x) + b_v \Delta\sigma_{SAR}^{c_v}(x)}{a}\right]^{\frac{1}{b}} \left[\frac{1}{(x - x_0)}\right]^{c_e} & x \in [x_0 + \varepsilon, x_0 + w] \\ 0 & otherwise \end{cases} \quad (2)$$

where $\Delta\sigma_{SAR}=\sigma^0-\sigma_{SAR}$ [dB], the parameters a, b, b_v, c_v and c_e are regressive coefficients, ε is introduced to prevent the singularity in $x=x_0$, being x_0 the near-range edge of the rain cloud with w its cross-track width. In [1] we have estimated the regressive coefficients being 0.0089, 2.4595, 0.1216, 3.8979 and -0.0230, respectively, using the hurricane case study, and in this work we have decided to re-use them and evaluate their performances on other study cases.

MREA rain estimation algorithm requires the X-SAR surface response in absence of precipitation, expressed by σ^0. Ideally this parameter should be given by a clear-sky observation of the scene of interest, very close in time to the case study and in the same geometrical and instrumental conditions. In absence of a suitable "background" image, in [1] we have estimated σ^0 by using rain-free pixels within X-SAR scene itself and supposed it constant all over the scene. SIDOC methodology allows improving and differentiating the estimation of X-SAR ground responses: in particular σ^0 for the classified "precipitation" pixel is estimated as the mean of values belonging to the same land-cover class. Reference [12] briefly analyses the performance of this method respect the [1] one for two Italian study cases.

4. RESULTS ANALYSIS

Figure 4 shows two rain rate maps for the November 5th case study, the right one obtained by WR data processed with standard Marshall-Palmer algorithm, while the left one is obtained with the methodology proposed in this work. The similitude between MREA estimations and WR measurements is evident both morphologically and numerically, nevertheless several important differences exist, for example MREA shows an area of precipitation absent in WR map, while a peak of WR map is quite negligible in CSK one. Finally the peak present in both map appears translate. Tab. I confirms these qualitative observations. It is worth to notice that respect [1] scene, this case is much more difficult, due to a complex orography that impacts on both instruments in a different way and due to the time difference between WR and CSK data.

Table I. Liguria (IT) Event Case: error analysis between MREA and WR Marshall-Palmer precipitation rates.

Mean	*Std*	*RMSE*	*Corr.*
-2.67	*10.35*	*10.69*	*12%*

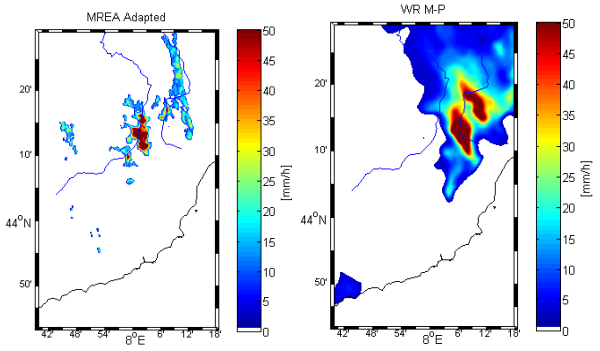

Figure 4. Liguria (IT) Event Case. (Left panel) CSK rain rate map obtained by the methodology proposed in this work. (Right panel) WR Marshall-Palmer (M-P) rain rate estimation over radar VMI.

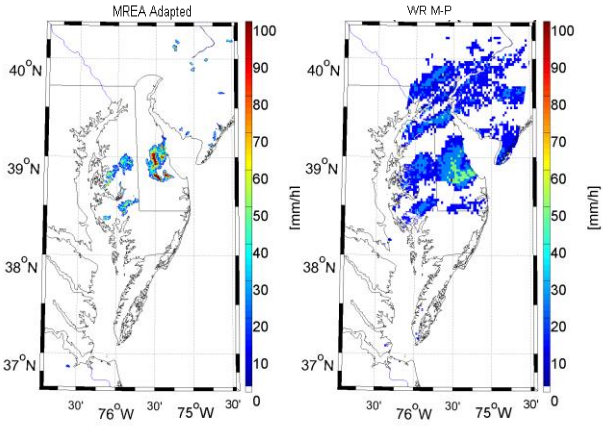

Figure 5. Hurricane "Irene" (U.S.) Event Case. (Left panel) CSK rain rate map obtained by the methodology proposed in this work. (Right panel) WR Marshall-Palmer (M-P) rain rate estimation over radar VMI.

Fig. 5 and Tab. II are the same of Fig. 4 and Tab. I for the other study case. Here orography is absent and time difference between WR and CSK data is negligible, and actually performances are better. Differences appear due to SIDOC parameters, perhaps a bit too restrictive, and to the tendency of MREA of over estimating precipitation rate.

Table II. Hurricane "Irene" (U.S.) Event Case: error analysis between MREA and WR Marshall-Palmer precipitation rates.

Mean	*Std*	*RMSE*	*Corr.*
-1.17	*6.39*	*6.50*	*40%*

5. CONCLUSIONS

The presented X_SAR CSK results are encouraging, even though more quantitative analyses are necessary regarding the effects of orography, spatial resolution degradation and inhomogeneous beam filling of precipitation fields on physical hydrologic analyses. The suggested X-SAR rainfall retrieval algorithm and classification algorithm need a systematic calibration and validation using other case studies.

Further developments are foreseen toward more sophisticated inversion methodologies, whereas better comprehension of spaceborne observed precipitations can arise from the use of mesoscale cloud models coupled with SAR response model and from the polarimetric capability of spaceborne XSARs and ground-based WR sensors. The proposed technique of X-SAR rainfall algorithm calibration uses Weather Radar measurements. An appealing idea is to design a synergetic approach between X-SAR and geostationary weather satellites with the purpose to develop a fully spaceborne framework for X-SAR Earth observations. These issues need to be still investigated and will be the objective of future works

6. ACKNOWLEDGEMENTS

The authors would like to acknowledge the ASI CSK Science Team for providing CSK data under the "RainXSAR" proposal (AO COSMOSkyMed). NCDC-NOAA is gratefully acknowledged for providing NEXRAD weather radar data and software tools (www.ncdc.noaa.gov/oa/wct), National Department of Civil Protection, Rome (Italy) for providing C-band radar data through the "IDRA2" project. This work has been partially supported by the National Department of Civil Protection, Rome (Italy) and by Sapienza University of Rome (Italy).

7. REFERENCES

[1] Marzano, F.S., Mori, S., Chini, M., Pulvirenti, L., Pierdicca, N., Montopoli, M. & Weinman, J.A. (2011). Potential of high-resolution detection and retrieval of precipitation fields from X-band spaceborne synthetic aperture radar over land, *Hydrology and Earth System Sciences*, **15**, 859-875.

[2] Danklmayer, A., Doring, B., Schwerdt, M. & Chandra, M. (2009). Assessment of atmospheric propagation effects in SAR, *IEEE Trans. Geosci. Rem. Sensing*, **47**, 3507-3518.

[3] Baldini, L., Fritz, J., Gorgucci, E. & Chandrasekar, V. (2010). Interpretation of satellite observations of precipitation using C-band polarimetric radar data, *Proc. ERAD 2010*, Sibiu (RO), 6-10 September.

[4] Marzano, F.S., Mori, S., Montopoli, M. & Weinman, J.A. (2012). Modeling Polarimetric Response of Spaceborne Synthetic Aperture Radar due to Precipitating Clouds from X to Ka band, *IEEE Trans. Geosci. Rem. Sens.*, **50**(3), 687-703.

[5] Covello, F., Battazza, F., Coletta, A., Lopinto, E., Fiorentino, C., Pietranera, L., Valentini, G., & Zoffoli, S. (2010). COSMO-SkyMed an existing opportunity for observing the Earth, *J. Geodyn*, **49**, 171-180.

[6] Werninghaus, R. Buckreuss, S. (2010). The TerraSAR-X Mission and System Design, *IEEE Trans. Geosci. Rem. Sensing*, **48**, 606-614.

[7] Vulpiani, G., Gioia, A., Giordano, P., Negri, M., Rossi, L., Pagliara, P., Alberoni, P.P., Amorati, R., Celano, M., Fornasiero, A., Poli, V., Cremonini, R., Ferraris, L., Montopoli, M., Rebora, N., Picciotti, E., Siccardi, F., Silvestro, F., & Marzano, F.S. (2008). The Italian radar network within the national early-warning system for multi-risks management, *Proc. ERAD08*, Helsinki (FL), 30-4 July.

[8] Lixion, A.A. & Cangialosi, J. (2012). Tropycal cyclone report – Hurricane Irene (AL092011), http://www.nhc.noaa.gov/data/tcr/AL092011_Irene.pdf

[9] Fulton, R.A., Breidenbach, J.P., Seo, D.-Jun, Miller, D.A., & O'Bannon, T. (1998). The WSR-88d Rainfall Algorithm, *Weather and Forecasting*, **13**, 377-395.

[10] Bringi, V.N., & Chandrasekar, V. (2001). Polarimetric Doppler Weather Radar, 1st ed., New York, USA, Cambridge university press.

[11] Pulvirenti, L., Marzano, F.S., Pierdicca, N., Mori, S. & Chini, M. (accepted). Discrimination of water surfaces, heavy rainfall and wet snow using COSMO-SkyMed observations of severe weather events, *IEEE Trans. Geosci. Rem. Sensing*.

[12] Mori, S., Pulvirenti, L., Chini, M., Pierdicca, N., Montopoli, M., Parodi, A., Weinman, J.A. & Marzano, F.S. (2012). Analysis of Rainfall Signatures on Cosmo-Skymed X-Band Synthetic Aperture Radar Observations, *Proc. of IEEE International Geoscience and Remote Sensing Symposium (IGARSS)*, Munich (D), 22-27 July.